Chirping the probe pulse in a coherent transients experiment

Sébastien Weber,* Bertrand Girard, and Béatrice Chatel
CNRS-Université de Toulouse, UPS, Laboratoire Collisions, Agrégats Réactivité, IRSAMC, F-31062 Toulouse, France
(Received 18 December 2009; published 18 February 2010)

Coherent transients occur when a chirped pump pulse excites a two-level transition. They have been observed with an ultrashort probe pulse. Several studies have been dedicated to using various pump shapes. In this study, the roles of the pump and the probe pulses are reversed. With a Fourier-transform-limited pump pulse followed by a chirped-probe pulse, similar effects can be observed. Finally, the case of two pulses with opposite chirps is considered.

DOI: 10.1103/PhysRevA.81.023415 PACS number(s): 42.50.Md, 42.65.Re, 32.80.Qk, 32.80.Rm

I. INTRODUCTION

For more than 20 years, the pump-probe technique has been one of the most powerful experimental techniques used to elucidate time-resolved dynamics using ultrashort lasers [1]. In a typical pump-probe experiment, the pump laser initiates the dynamics by exciting a combination of states. To measure the temporal evolution, a probe pulse is used to lead the system to a final state, producing a signal which reveals the dynamics induced as a function of the pump-probe delay. Quite early on, some work has been done theoretically [2] as well as experimentally to emphasize the role of the probe. In particular it has been shown that a careful adjustment of the wavelength in wave-packet dynamics studies can give access to different pathway [3–5]. Also, changing the probe polarization allows one to observe different dynamics [6,7]. In parallel, the advent of pulse shaping [8] has led to fascinating results in coherent control [9–11]. Many of these results have been obtained by manipulating the shape of the pump pulse [12–20]. Some results have been obtained by shaping the spectral phase of the probe in order to select the final state in Li_2 [21] or to exhibit vibrational dynamics in the liquid phase [22]. Moreover, shaping the probe in phase or in polarization has been widely implemented in coherent anti-Stokes Raman spectroscopy (CARS) experiments [23–25] to drastically reduce the nonresonant background as well as to significantly enhance the resonant CARS signal. This process also leads to a huge improvement in both the sensitivity and the spectral resolution. Interesting implementations have been performed, including both coherent control and interferometry techniques to simplify the CARS setup by single-pulse phase-control nonlinear Raman spectroscopy [25]. In the same way, chirped probes have been used to improve the spectral resolution [26] using their time-spectral homothetic transformation properties [27] and also to show theoretically the gain of information about molecular properties [28]. At the same time, we have studied in great detail the interaction of a chirped pump with a two-level system [29]. The evolution of the population amplitude has been studied using an ultrashort probe. Contrary to the CARS scheme, here a two-photon transition with an intermediate state close to the one-photon transition is considered. We propose to study the effect of a chirped probe in such a scheme. A detailed comparative analysis is performed between the normal chirped-pump pulse and Fourier-Transform-Limited (FTL) probe pulse case and the reversed case with a FTL pump and a chirped-probe pulse. Thus, we emphasize that the probe plays a crucial role in the dynamics, not only by fixing the analysis resolution but also by determining the temporal evolution behavior itself. Finally we demonstrate that, for particular values of the probe and pump spectral phases, one can obtain a short dynamic even with pump and probe that are long. Moreover, it can be a way to measure the spectral phase of the electric field.

II. PRINCIPLE

In this paper, a pump-probe scheme is considered within a three-level system. Each pulse is resonant with only one transition. The two transitions are excited successively by two pulses. These pulses can generally be shaped. However, only the cases where one of the pulses is FTL and the other one is highly chirped are considered in this section. To understand these dynamics, we first recall the interaction of a chirped pulse with a two-level system (Sec. II A). The evolution of the excited-state probability amplitude is described during this interaction. Then the case of a chirped-pump pulse followed by an ultrashort pulse is examined (already addressed in previous studies [27,29–32]; see Sec. II B), which probes the dynamics in the excited state. Finally the case of a chirped probe preceded by an ultrashort pump pulse, which triggers the dynamics (Sec. II C), is studied. Although the physical situations are different, these two cases lead to similar behaviors as a function of the delay.

A. Interaction of a two-level system with a chirped pulse

In the temporal domain, the chirped pulse of duration T_C and angular frequency ω_C is written as

$$E_C(t) = \mathcal{E}_0 \sqrt{\frac{T_0}{T_C}}\, e^{-t^2/T_C^2}\, e^{-i(\omega_C t - \alpha t^2)}, \tag{1}$$

where T_C and α are related to the chirp rate ϕ'' by

$$T_C = T_0 \sqrt{1 + \left(\frac{2\phi''}{T_0^2}\right)^2}, \quad \alpha = \frac{2\phi''}{T_0^4 + (2\phi'')^2} \tag{2}$$

and T_0 is the duration of the corresponding FT-limited pulse.

The lower and upper states are denoted $|g\rangle$ and $|e\rangle$ (for ground and excited states), respectively. First-order

*sebastien.weber@irsamc.ups-tlse.fr

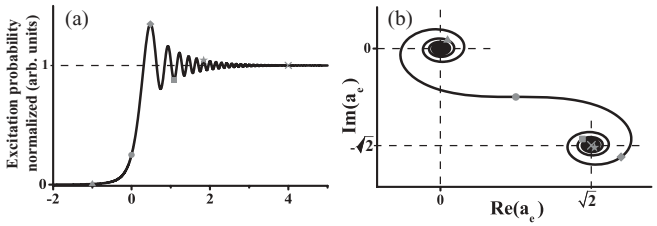

FIG. 1. Evolution of the upper-state population under the excitation of a chirped pulse: (a) probability exhibiting coherent transient normalized to unity for long time and (b) corresponding probability amplitude in the complex plane. The symbols correspond to different values of time τ: -1000 fs (triangle), 0 fs (circle), 480 fs (diamond), 1090 fs (square), 1840 fs (star), and 4000 fs (cross).

perturbation theory gives the excited-state probability amplitude during the resonant interaction ($\omega_C \simeq \omega_{eg}$) with the chirped pulse:

$$a_e(t) = -\frac{\mu_{eg}}{2\hbar}\int_{-\infty}^{t} E_c(t)\, e^{i\omega_{eg}t'}\, dt' = -\frac{\mu_{eg}}{2\hbar}\int_{-\infty}^{t} \mathcal{E}_0\sqrt{\frac{T_0}{T_p}}\, e^{-t'^2/T_C^2}\, e^{i(\omega_{eg}-\omega_C)t'}\, e^{-i\alpha t'^2} dt'. \quad (3)$$

The result of this interaction has been studied in detail [29] and is sketched in Fig. 1. The probability amplitude during this interaction follows a Cornu spiral (equivalent to the diffraction by a knife edge) in the complex plane [Fig. 1(b)]. The excitation probability [Fig. 1(a)] presents a large increase when the instantaneous frequency goes through resonance. It is followed by oscillations which can be interpreted as beats between the atomic dipole excited at resonance and the instantaneous frequency which is shifting away from resonance. These oscillations are due to the quadratic phase which appears in the integral given by Eq. (4).

B. Chirped-pump pulse and FTL-probe pulse

In the scheme studied in previous works, the dynamics is observed in real time with a second ultrashort pulse as a probe. Therefore, the simplest pump-probe scheme is considered within a three-level system. These levels are the ground, excited, and final states and are denoted $|g\rangle$, $|e\rangle$, and $|f\rangle$, respectively, as shown in Fig. 2. The two sequential transitions $|g\rangle \rightarrow |e\rangle$ and $|e\rangle \rightarrow |f\rangle$ are respectively excited by a pump pulse $E_{\mathrm{pu}}(t)$ of carrier angular frequency ω_{pu} close to resonance ($\delta_{\mathrm{pu}} = \omega_{eg} - \omega_{\mathrm{pu}}$, $|\delta_{\mathrm{pu}}| \ll \omega_{eg}$), centered on $t = 0$, and by a probe pulse $E_{\mathrm{pr}}(t)$ of carrier angular frequency ω_{pr} close to resonance ($\delta_{\mathrm{pr}} = \omega_{fe} - \omega_{\mathrm{pr}}$, $|\delta_{\mathrm{pr}}| \ll \omega_{fe}$) and centered on $t = \tau$. The fluorescence arising from the $|f\rangle$ state can be recorded as a function of the pump-probe delay τ. The observed signal is proportional to the population $|a_f(\tau)|^2$ in the final state $|f\rangle$. The general expression of the probability amplitude $a_f(\tau)$ to find the system in the final state is given

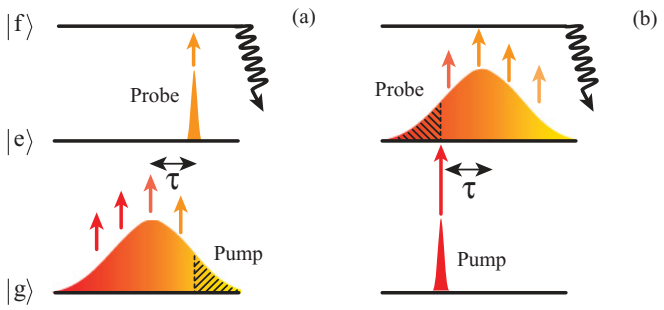

FIG. 2. (Color online) Principle of the excitation scheme. (a) In the case of a chirped pump and a short probe, the probe "freezes" the interaction at time τ. (b) In the case of a short pump and a chirped probe, the pump triggers the interaction between the chirped pulse and the upper two levels at time $-\tau$ (with respect to the chirped pulse).

by the second-order perturbation theory:

$$a_f(\tau) = -\frac{\mu_{fe}\mu_{eg}}{4\hbar^2}\int_{-\infty}^{+\infty} dt' E_{\mathrm{pr}}(t'-\tau) e^{i\omega_{fe}(t'-\tau)} \times \int_{-\infty}^{t'} dt\, E_{\mathrm{pu}}(t) e^{i\omega_{eg}t}. \quad (4)$$

In the first case, the pump pulse is chirped $E_{\mathrm{pu}}(t) = E_C(t)$. The probe pulse is ultrashort and FTL. This scheme is depicted in Fig. 2(a). The interaction takes place from the beginning of the chirped pulse until time τ, when the ultrashort probe is applied. For a probe much shorter than the dynamics induced in the system, we can consider it a Dirac $E_{\mathrm{pr}}(t-\tau) \propto \delta(t-\tau)$ and simplify Eq. (4). We obtain an expression similar to the resonant interaction of a chirped pulse with a two-level system [Eq. (4)], except that τ is now the pump-probe delay instead of the real time of the chirped pulse. One gets

$$a_f(\tau) \simeq -\frac{\mu_{fe}\mu_{eg}}{4\hbar^2}\int_{-\infty}^{\tau} dt\, E_{\mathrm{pu}}(t) e^{i\omega_{eg}t}. \quad (5)$$

The final-state population $|a_f(\tau)|^2$ as a function of the pump-probe delay τ is therefore similar to the real-time temporal evolution of the level $|e\rangle$ in the two-level case, as displayed in Fig. 1 and already widely studied [29] and manipulated [18,27,30].

C. FTL-pump pulse and chirped-probe pulse

We consider here the case of an ultrashort FTL-pump pulse followed by a chirped-probe pulse. The ultrashort pump pulse can also be approximated by a Dirac so that

$$a_f(\tau) \simeq -\frac{\mu_{fe}\mu_{eg}}{4\hbar^2}\int_{-\infty}^{+\infty} dt' E_{\mathrm{pr}}(t'-\tau) e^{i\omega_{fe}(t'-\tau)} \times \int_{-\infty}^{t'} dt\, \delta(t) e^{i\omega_{eg}t} \quad (6)$$

with

$$\int_{-\infty}^{t'} dt\delta(t)e^{i\omega_{eg}t} = \begin{cases} 1 & \text{for} \quad t' > 0, \\ 0 & \text{for} \quad t' < 0. \end{cases}$$

Then

$$a_f(\tau) \simeq -\frac{\mu_{fe}\mu_{eg}}{4\hbar^2}\int_0^{+\infty} dt' E_{\rm pr}(t'-\tau)e^{i\omega_{fe}(t'-\tau)}$$
$$\simeq -\frac{\mu_{fe}\mu_{eg}}{4\hbar^2}\int_{-\tau}^{+\infty} dt' E_{\rm pr}(t')e^{i\omega_{fe}(t')}, \qquad (7)$$

which means that in this case the dynamics induced by the chirped pulse between the two upper levels is triggered by the pump [cf. Fig. 2(b)]. Although Eq. (7) is similar to the previous case [Eq. (5)], the interpretation of the observed oscillations is less straightforward. Indeed, the observed signal is not directly related to the dynamics of the upper level (here $|f\rangle$) excited by the chirped pulse. Modifying the value of τ changes only the starting time of the dynamics. The measured signal is the final result, at the end of these dynamics.

To better explain the difference between the delay τ and the real time t in this situation, Fig. 3 presents a two-dimensional plot of the $|f\rangle$ state population as a function of time t and delay τ. A horizontal cut corresponds to the real-time dynamics in the upper state. Several of such cuts (along the horizontal dashed lines in Fig. 3) correspond to the temporal evolution for a given pump-probe delay. They are displayed in the left-hand side of Fig. 4. A vertical cut at a time longer than the chirped-pulse duration corresponds to the final population as a function of the delay τ (see Fig. 3, right-hand side). The same oscillations are predicted as for the usual coherent transients. Indeed,

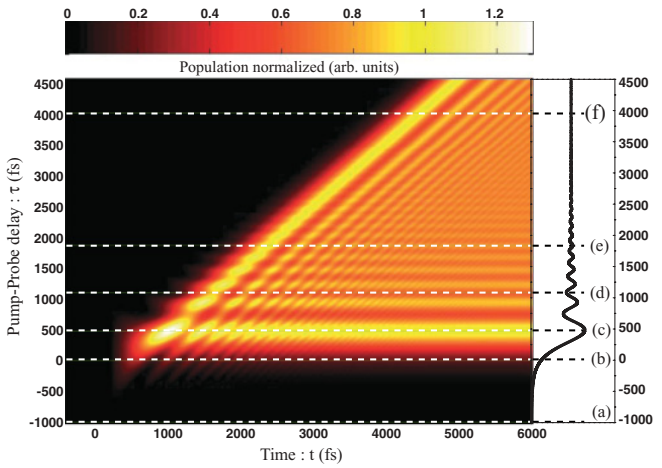

FIG. 3. (Color online) Two-dimensional mapping of the final-state population (normalized to the population at long time and delay). The vertical axis is the delay between the pump and the probe (τ in the equations), and the horizontal axis is the time evolution (t in the equations). A vertical cut at 6 ps is plotted on the right-hand side, corresponding to the evolution of the asymptotic value of the final population. This value is the one measured via the experiment. Several horizontal dashed lines are plotted, which correspond to the different cases presented in Fig. 4.

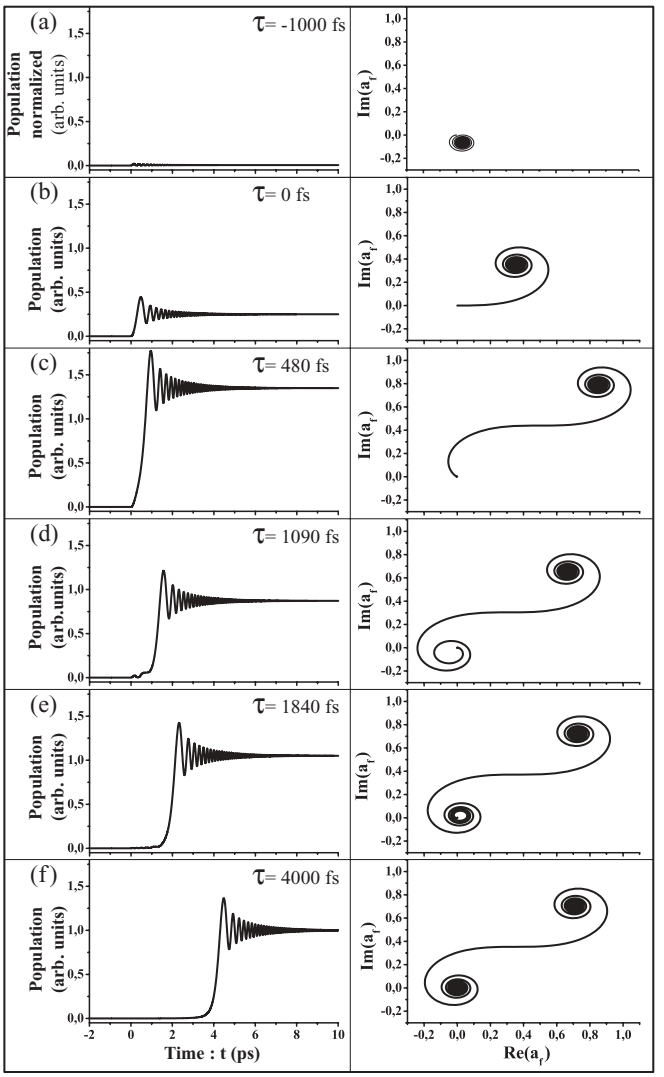

FIG. 4. Left: Temporal evolution of the final population during the probe pulse [normalized to the population at long time and delay; see case (f)]. Right: Corresponding probability amplitude plotted in the complex plane. Pump-probe delays are (a) −1000, (b) 0, (c) 480, (d) 1090, (e) 1840, and (f) 4000 fs.

Eqs. (5) and (7) are completely similar if the pump and probe spectral phases are inverted.

Another way to understand these predictions is to plot, in the complex plane, the temporal evolution of the probability amplitudes in the $|f\rangle$ state (right-hand panels of Fig. 4) for various delays. For the largest delay, $\tau = 4000$ fs [Fig. 4(f)], the pump pulse arrives long before the chirped pulse so that the whole dynamics can take place. One can see the Cornu spirals again, starting from the origin and finishing at the asymptotic value which corresponds to the measured quantity. On the left-hand panel, the population exhibits the same coherent transients as in the usual situation (see Fig. 1). At the opposite, for large negative values of τ, the probe arrives before the pump and the signal (left) is negligible. Moving now from large positive values to shorter delays ($\tau = 1840$, 1090, and 480 fs for Figs. 4(e), 4(d), and 4(c), respectively), a progressively larger fraction of the leading part of the chirped pulse is inactive. Thus, part of the beginning of

the spiral is suppressed. In the complex plane, the curve starts always from the origin. Therefore, the truncated spiral must be shifted. The new starting points are shown by symbols in Fig. 1(b). The remaining curve is therefore shifted. The final point is alternatively further, closer, and further from the origin, corresponding to maxima and minima of the asymptotic values and therefore of the upper-state population (left). One should notice that although there are strong similarities with Coherent Transients (CT), these curves are not. In particular, small oscillations are observed before the rising edge [see, for instance, Fig. 4(d)]. This is a consequence of the truncated spiral. At $\tau = 0$, the pump pulse is at the maximum of the chirped pulse. Exactly half of the spiral is left. The final probability amplitude is half of that reached for largest values of τ and the population is one-fourth. Finally, for negative delays, very weak oscillations are observed.

Another way to explain these behaviors is to notice that the population is simply the square of the distance between the starting and final points of the evolution of the probability amplitude. Therefore, only the relative evolution is meaningful and it is not necessary to center the starting point of the truncated spiral at the origin. Each curve in Fig. 4 (left) is therefore obtained by plotting the square of the distance between an arbitrary origin on the spiral (corresponding to the value of the delay τ) and a point moving on the spiral. This explains more clearly why oscillations are obtained before the rising edge, when both starting and final points are within the same part of the spiral in Fig. 4(d) (left).

When considering the asymptotic value (in other words, the observed pump-probe signal), it is also simpler to consider that the final point of the spiral is fixed. Thus, changing the delay τ (from $+\infty$ to $-\infty$) is simply equivalent to removing progressively larger parts of the spiral. One fully understands why the situation (for the pump-probe signal) is exactly symmetric to the first case when the pump is chirped.

III. EXPERIMENTAL RESULTS

To illustrate this point, an experiment has been performed in an atomic Rb vapor (Fig. 5). The Rb [$5s$-$5p(P_{1/2})$] transition (at 795 nm) is almost resonantly excited with an ultrashort pump pulse. (The laser spectrum is centered around 808 nm with a full width at half maximum of 24 nm.)

The transient excited-state population is probed "in real time" on the [$5p$-($8s$, $6d$)] transitions with a pulse produced by a homemade noncolinear optical parametric amplifier (603 nm, 25 fs). This probe pulse is negatively chirped ($\phi''_{\rm pr} = -1.4 \times 10^5$ fs^2) by a pair of gratings, recombined with the pump pulse, and sent into a sealed rubidium cell with fused-silica Brewster-window ends [18,29,30]. The pump can be shaped using a high-resolution pulse shaper [33] formed by a double liquid-crystal spatial light modulator (640 pixels) placed in a Fourier plane of a highly dispersive $4f$ line. Care should be taken to block the red part of the spectrum in order to avoid any two-photon transition (at 778 nm) and spin-orbit oscillations (at 780 nm) [34]. The pump-probe signal is detected by monitoring the fluorescence at 420 nm due to the radiative cascade $(ns, n'd) \rightarrow 6p \rightarrow 5s$. As expected, strong oscillations appear clearly as the black dots of the curve in Fig. 6 when the probe is chirped. These oscillations are

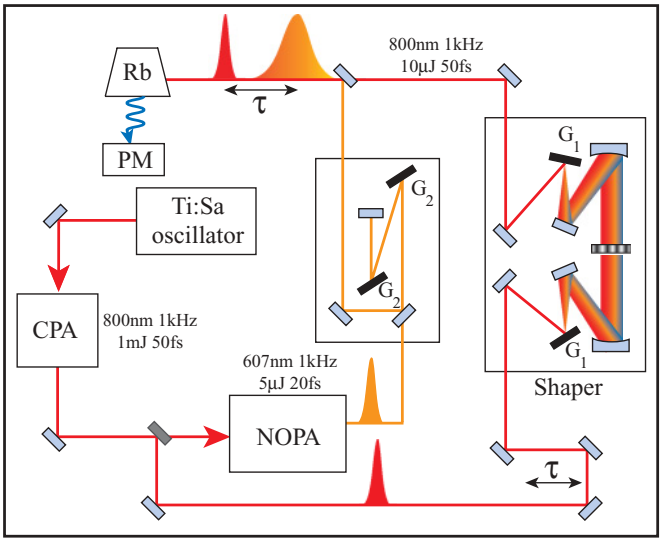

FIG. 5. (Color online) Experimental setup: G2, gratings with 600 grooves/mm. G1, gratings with 2000 grooves/mm. NOPA, noncolinear optical parametric amplifier.

similar to the coherent transients observed previously with the chirped pump [29]. The contrast is excellent and experimental data (black dots) fit well with the theoretical data (gray solid line) obtained by analytical resolution of Eq. (4).

To demonstrate the interplay of the pump and the probe, different amounts of chirp are applied on the pump pulse using the shaper. Equation (4) can be calculated exactly and leads to a rather complex expression in the general case of nonzero detunings (which is the case here) [35]:

$$a_f(\tau) \propto \frac{1}{\sqrt{\beta_{\rm pu}\beta_{\rm pr}}}\left[1 - \mathrm{erf}\left(-\frac{\gamma\sqrt{\beta_{\rm pu}+\beta_{\rm pr}}}{2\sqrt{\beta_{\rm pu}\beta_{\rm pr}}}\right)\right],$$
$$\gamma = \frac{i(\beta_{\rm pu}\delta_{\rm pr} - \beta_{\rm pr}\delta_{\rm pu}) - 2\beta_{\rm pu}\beta_{\rm pr}\tau}{\beta_{\rm pu}+\beta_{\rm pr}} \tag{8}$$

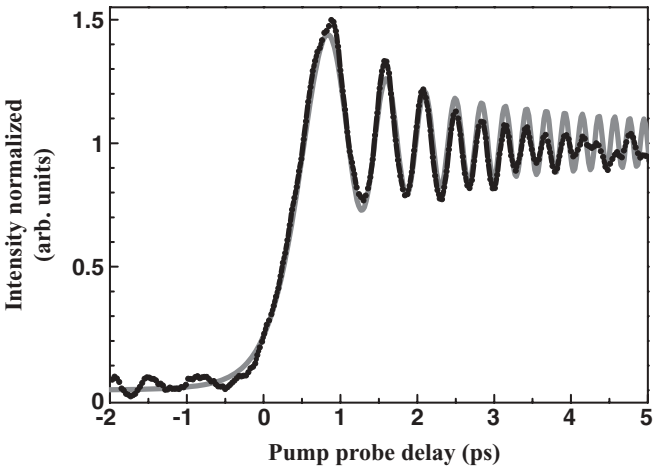

FIG. 6. Experimental coherent transients on Rb ($5s$-$5p$ at 795 nm), for a chirp of $\phi''_{\rm pr} = -1.4 \times 10^5$ fs^2 on the probe (black dots) and the corresponding simulation obtained by numerical resolution of the Schrödinger equation (solid gray line). Curves are normalized to unity at long time.

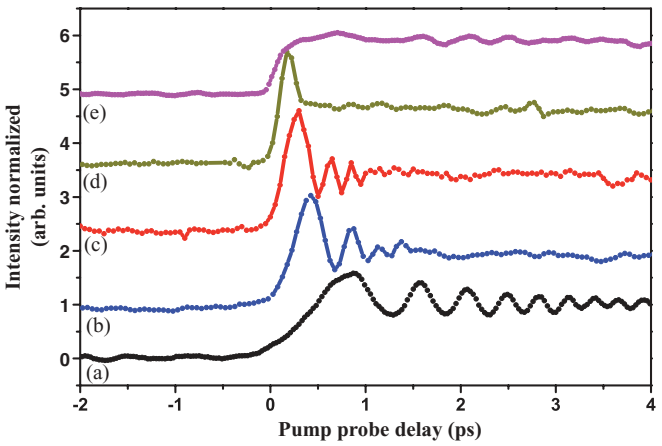

FIG. 7. (Color online) Experimental coherent transients measured for a chirp of $\phi''_{pr} = -1.4 \times 10^5$ fs^2 on the probe and sequential chirp values for the pump (ϕ''_{pu}). Curves are normalized to unity at long time and shifted vertically for clarity. The (a) black-dot solid curve corresponds to transients obtained with a FT-limited pump (see Fig. 6) plotted here for comparison: (b) $\phi''_{pu} = 1.0 \times 10^5$ fs^2 (blue), (c) $\phi''_{pu} = 1.2 \times 10^5$ fs^2 (red), (d) $\phi''_{pu} = 1.4 \times 10^5$ fs^2 (green), and (e) $\phi''_{pu} = 1.5 \times 10^5$ fs^2 (purple). The increasing chirp of the pump gives fewer oscillations in the transients. For opposite chirps (d), the oscillations are completely removed [such as for curve (e)], but the rising time obtained is here the shortest. It is equivalent to the FT-limited cross-correlation duration. The sharp peak around $\tau = 0$ is due to the detuning of the central laser wavelength with respect to the resonance wavelength.

where $\beta_k = \frac{1}{T_{C,k}^2} + i\alpha_k$, δ_k (k = pu, pr), is the detuning of the two pulses with respect to their transition frequencies and erf is the error function. The complex part of the argument of the erf function is responsible for the oscillations while the real part sets the rising time. Setting fixed the chirp of the probe and varying the chirp of the pump, the evolution of the final state could be drastically changed (see Fig. 7).

An interesting case is the one where chirp on the pump and the probe are opposite and fulfill the condition $\phi''_k \gg T_{0,k}^2$. One gets the simplified expression for identical bandwidths ($T_{0,pu} = T_{0,pr} = T_0$):

$$a_f(\tau) \propto T_0\, T_C \left[1 - \mathrm{erf}\left(-\frac{\tau}{\sqrt{2}T_0} + \eta\right)\right],$$
$$\eta = -\frac{(\phi''_{pu}\delta_{pr} + \phi''_{pr}\delta_{pu})}{\sqrt{2}T_0} + i\frac{T_0}{2\sqrt{2}}(\delta_{pr} - \delta_{pu}). \quad (9)$$

Two comments can be addressed:

1. For zero detuning $\delta_k = 0$, the evolution of $a_f(\tau)$ is a simple step with a rising time equal to $\sqrt{2}T_0$. The oscillations are vanishing. The obtained dynamics is the same as with two FT-limited pulses. $\sqrt{2}T_0$ is their cross-correlation duration.

2. In the general case with detuning, η [Eq. (9)] is a complex number. Its real part delays the step while its complex part gives a sharp peak around $\tau = 0$, which is well known as the cross-correlation peak [36] [see Fig. 7(d)].

Experimental data are presented in Fig. 7 with $\phi''_{pr} = -1.4 \times 10^5$ fs^2 ($T_C \simeq 10$ ps) on the probe and (a) $\phi''_{pu} = 0$ fs^2, (b) $\phi''_{pu} = 1.0 \times 10^5$ fs^2, (c) $\phi''_{pu} = 1.2 \times 10^5$ fs^2, (d) $\phi''_{pu} = 1.4 \times 10^5$ fs^2, and (e) $\phi''_{pu} = 1.5 \times 10^5$ fs^2. Due to laser constraint, there is a large detuning on the pump. However, one can see that the oscillations of the transients are vanishing when chirps on the pump and probe become opposite [cases (d) and (e)]. As predicted by Eq. (9), the cancellation of the chirps leads to the shortest rising time of the pump probe signal, of the order of 60 fs [case (d)]. For case (e), the evolution is a simple step with no peak and no oscillations despite the large detuning of the laser. This behavior can be explained, especially the absence of the sharp peak, by a fine balance between chirp and detuning in the complex time-dependent part of γ [Eq. (8)]. Thus, the best criterion for chirp compensation is not the cancellation of the oscillations but the sharpness of the slope. The sensitivity of the coherent transients could thus be used as a fine adjustment of the pump chirp. This value is determined here with an accuracy of 10%, but this can certainly be improved.

This method could be used to determine the spectral phase of an unknown pulse. This approach will be particularly appropriate when one of the pulses is in a spectral range where it cannot be easily characterized. Further work is under way to see how the combination of complex spectral phases for both pump and probe pulses can be used as a useful tool for time-resolved spectroscopies.

IV. CONCLUSION

In this paper we have demonstrated how the phase of the probe pulse could significantly affect the pump-probe signal, in a way equivalent to that of the phase of the pump. An illustrative experiment has been performed in rubidium vapor. Indeed, the spectral phases of the two pulses contribute equally, which was clearly demonstrated with two pulses of opposite chirp. A pump-probe signal with a very short rising time followed by a plateau has been obtained even with strongly chirped pump and probe pulses. This finding opens the door toward new pump-probe schemes where both pump and probe spectral phases can be shaped. It should be noted that this situation is the opposite of sum-frequency generation. Indeed, it was observed in this latter case [37,38] that a long pulse with narrow bandwidth is generated. The presence of the resonant intermediate level creates the short transient.

ACKNOWLEDGMENTS

We sincerely acknowledge Elsa Baynard for her technical help and Chris Meier and Sébastien Zamith for fruitful discussions. This work was supported by the Agence Nationale de la Recherche (Contract No. ANR-06-BLAN-0004) and the Marie Curie Initial Training Network Grant No. CA-ITN-214962-FASTQUAST.

[1] A. H. Zewail, *Femtochemistry: Ultrafast Dynamics of the Chemical Bond* (World Scientific, Singapore, 1994), Vols. I and II.
[2] H. Metiu and V. Engel, J. Chem. Phys. **93**, 5693 (1990).
[3] C. Nicole, M. A. Bouchene, C. Meier, S. Magnier, E. Schreiber, and B. Girard, J. Chem. Phys. **111**, 7857 (1999).
[4] H. Katsuki, H. Chiba, B. Girard, C. Meier, and K. Ohmori, Science **311**, 1589 (2006).
[5] H. Katsuki, H. Chiba, C. Meier, B. Girard, and K. Ohmori, Phys. Rev. Lett. **102**, 103602 (2009).
[6] S. Zamith, M. A. Bouchene, E. Sokell, C. Nicole, V. Blanchet, and B. Girard, Eur. Phys. J. D **12**, 255 (2000).
[7] E. Sokell, S. Zamith, M. A. Bouchene, and B. Girard, J. Phys. B **33**, 2005 (2000).
[8] A. M. Weiner, Rev. Sci. Instrum. **71**, 1929 (2000).
[9] A. Assion, T. Baumert, M. Bergt, T. Brixner, B. Kiefer, V. Seyfried, M. Strehle, and G. Gerber, Science **282**, 919 (1998).
[10] T. C. Weinacht, J. Ahn, and P. H. Bucksbaum, Phys. Rev. Lett. **80**, 5508 (1998).
[11] J. L. Herek, W. Wohlleben, R. J. Cogdell, D. Zeidler, and M. Motzkus, Nature **417**, 533 (2002).
[12] D. Meshulach and Y. Silberberg, Nature **396**, 239 (1998).
[13] N. Dudovich, B. Dayan, S. M. Gallagher Faeder, and Y. Silberberg, Phys. Rev. Lett. **86**, 47 (2001).
[14] P. Balling, D. J. Maas, and L. D. Noordam, Phys. Rev. A **50**, 4276 (1994).
[15] B. Chatel, J. Degert, and B. Girard, Phys. Rev. A **70**, 053414 (2004).
[16] R. Netz, A. Nazarkin, and R. Sauerbrey, Phys. Rev. Lett. **90**, 063001 (2003).
[17] M. Wollenhaupt, A. Prakelt, C. Sarpe-Tudoran, D. Liese, T. Bayer, and T. Baumert, Phys. Rev. A **73**, 063409 (2006).
[18] A. Monmayrant, B. Chatel, and B. Girard, Phys. Rev. Lett. **96**, 103002 (2006).
[19] K. Ohmori, Annu. Rev. Phys. Chem. **60**, 487 (2009).
[20] A. Präkelt, M. Wollenhaupt, C. Sarpe-Tudoran, and T. Baumert, Phys. Rev. A **70**, 063407 (2004).
[21] X. Dai and S. Leone, J. Chem. Phys. **127**, 014312 (2007).
[22] D. Polli, D. Brida, G. Lanzani, and G. Cerullo, Conference on Lasers and Electro-Optics/International Quantum Electronics Conference (CLEO/IQEC) (2009).
[23] N. Dudovich, D. Oron, and Y. Silberberg, Nature **418**, 512 (2002).
[24] D. Oron, N. Dudovich, D. Yelin, and Y. Silberberg, Phys. Rev. Lett. **88**, 063004 (2002).
[25] Y. Silberberg, Annu. Rev. Phys. Chem. **60**, 277 (2009).
[26] K. P. Knutsen, J. C. Johnson, A. E. Miller, P. B. Petersen, and R. J. Saykally, Chem. Phys. Lett. **387**, 436 (2004).
[27] W. Wohlleben, J. Degert, A. Monmayrant, B. Chatel, M. Motzkus, and B. Girard, Appl. Phys. B **79**, 435 (2004).
[28] P. Marquetand, P. Nuernberger, T. Brixner, and V. Engel, J. Chem. Phys. **129**, 074303 (2008).
[29] S. Zamith, J. Degert, S. Stock, B. de Beauvoir, V. Blanchet, M. A. Bouchene, and B. Girard, Phys. Rev. Lett. **87**, 033001 (2001).
[30] J. Degert, W. Wohlleben, B. Chatel, M. Motzkus, and B. Girard, Phys. Rev. Lett. **89**, 203003 (2002).
[31] A. Monmayrant, B. Chatel, and B. Girard, Opt. Lett. **31**, 410 (2006).
[32] A. Monmayrant, B. Chatel, and B. Girard, Opt. Commun. **264**, 256 (2006).
[33] A. Monmayrant and B. Chatel, Rev. Sci. Instrum. **75**, 2668 (2004).
[34] B. Chatel, D. Bigourd, S. Weber, and B. Girard, J. Phys. B **41**, 074023 (2008).
[35] S. Zamith, Ph.D. thesis, Université Paul Sabatier, 2001.
[36] I. V. Hertel and W. Radloff, Rep. Prog. Phys. **69**, 1897 (2006).
[37] F. Raoult, A. C. L. Boscheron, D. Husson, C. Sauteret, A. Modena, V. Malka, F. Dorchies, and A. Migus, Opt. Lett. **23**, 1117 (1998).
[38] K. Osvay and I. N. Ross, Opt. Commun. **166**, 113 (1999).